Inorg. Chem. **2003**, *42*, 3262–3273

Competition between Transferrin and the Serum Ligands Citrate and Phosphate for the Binding of Aluminum

Wesley R. Harris,* Zhepeng Wang, and Yahia Z. Hamada

Department of Chemistry and Biochemistry, University of Missouri−St. Louis, St. Louis, Missouri 63121

Received September 11, 2002

A key issue regarding the speciation of Al^{3+} in serum is how well the ligands citric acid and phosphate can compete with the iron transport protein serum transferrin for the aluminum. Previous studies have attempted to measure binding constants for each ligand separately, but experimental problems make it very difficult to obtain stability constants with the accuracy required to make a meaningful comparison between these ligands. In this study, effective binding constants for Al–citrate and Al–phosphate at pH 7.4 have been determined using difference UV spectroscopy to monitor the direct competition between these ligands and transferrin. The analysis of this competition equilibrium also includes the binding of citrate and phosphate as anions to apotransferrin. The effective binding constants are $10^{11.59}$ for the 1:1 Al–citrate complexes and $10^{14.90}$ for the 1:2 Al–citrate complexes. The effective binding constant for the 1:2 Al–phosphate complex is $10^{12.02}$. No 1:1 Al–phosphate complex was detected. Speciation calculations based on these effective binding constants indicate that, at serum concentrations of citrate and phosphate, citrate will be the primary low-molecular-mass ligand for aluminum. Formal stability constants for the Al–citrate system have also been determined by potentiometric methods. This equilibrium system is quite complex, and information from both electrospray mass spectrometry and difference UV experiments has been used to select the best model for fitting the potentiometric data. The mass spectra contain peaks that have been assigned to complexes having aluminum:citrate stoichiometries of 1:1, 1:2, 2:2, 2:3, and 3:3. The difference UV results were used to determine the stability constant for $Al(H_{-1}cta)^{-}$, which was then used in the least-squares fitting of the potentiometric data to determine stability constants for $Al(Hcta)^{+}$, $Al(cta)$, $Al(cta)_2^{3-}$, $Al(H_{-1}cta)(cta)^{4-}$, $Al_2(H_{-1}cta)_2^{2-}$, and $Al_3(H_{-1}cta)_3(OH)^{4-}$.

Introduction

Because aluminum is so abundant in the Earth's crust and is so widely used in modern technology, the general population is exposed to relatively high levels of this metal.[1,2] Healthy adults are well protected against toxicity from ingested aluminum by the very low absorption of this metal internally and by the efficient removal of Al^{3+} from the blood via the kidneys.[3,4] However, aluminum toxicity is observed when these protective mechanisms fail. This was most clearly demonstrated in the 1970s by the appearance of severe neurological disorders among long-term dialysis patients (dialysis dementia).[5,6] This effect was eventually linked to a combination of intestinal absorption of aluminum from phosphate-binding drugs and the transfer of aluminum from the dialysis solution across the dialysis membrane directly into the blood. Aluminum toxicity has also been observed in infants, whose kidney function is not fully developed.[7−9] There has been considerable debate over a possible role for aluminum in the development of Alzheimer's disease[10−13]

* To whom correspondence should be addressed. E-mail: wharris@umsl.edu.

(1) Martin, R. B. *Acc. Chem. Res.* **1994**, *27*, 204−210.
(2) Gregor, J. L. In *Aluminum in Biology and Medicine*; Chadwick, D. J., Whelan, J., Eds.; Wiley: New York, 1992; pp 26−49.
(3) Exley, C.; Burgess, E.; Day, J. P.; Jeffrey, E. H.; Melethil, S.; Yokel, R. A. In *Research Issues in Aluminum Toxicity*; Yokel, R. A., Golub, M. S., Eds.; Taylor & Francis: Washington, DC, 1996; pp 117−132.
(4) Ganrot, P. O. *Environ. Health Perspect.* **1986**, *65*, 363−441.
(5) Alfrey, A. C. *Contrib. Nephrol.* **1993**, *102*, 110−124.
(6) Kerr, D. N. S.; Ward, M. K.; Ellis, H. A.; Simpson, E. W.; Parkinson, I. S. In *Aluminum in Biology and Medicine*; Chadwick, D. J., Whelan, J., Eds.; Wiley: New York, 1992; pp 123−141.
(7) Hawkins, N. M.; Coffey, S.; Lawson, M. S.; Delves, H. T. *J. Pediatr. Gastroenterol. Nutr.* **1994**, *19*, 377−381.
(8) Klein, G. L. *Am. J. Clin. Nutr.* **1995**, *61*, 449−456.
(9) Freundlich, M.; Zilleruelo, G.; Abitbol, C.; Strauss, J. *Lancet* **1985**, 527−529.
(10) McLachlan, D. R.; Bergeron, C.; Smith, J. E.; Boomer, D.; Rifat, S. L. *Neurology* **1996**, *46*, 401−405.

10.1021/ic026027w CCC: $25.00
Published on Web 04/16/2003

and other neurological disorders, such as Parkinson's disease and amyotrophic lateral sclerosis.[4]

As the significance of aluminum toxicity has become apparent, considerable attention has been given to defining the chemical speciation of the Al^{3+} ion in human serum. Several fractionation studies have reported the distribution of Al^{3+} ions between proteins and low-molecular-mass (LMM) ligands. Most of the earlier studies reported that ~80% of the aluminum in serum was bound to proteins.[14−20] As methodologies have improved, this figure has tended to increase to ~90%.[21−27] It now appears that essentially all the high-molecular-mass aluminum in serum is bound to the iron transport protein transferrin.[22−24,26−31]

Transferrin consists of two similar lobes. Each lobe is further divided into two domains, with a high-affinity metal-binding site located within a cleft between the two domains. The Fe^{3+} ion in each lobe is coordinated to four ligands from protein side chains: two tyrosine phenolic groups, an imidazole group from one histidine residue, and the carboxylate side chain of an aspartic acid.[32,33] The fifth and sixth coordination sites on the Fe^{3+} ion are occupied by a bidentate carbonate anion derived from the buffer that is called the synergistic anion.

No crystal structure has been reported for the Al−transferrin complex, but it is highly likely that the Al^{3+} ion binds in essentially the same manner as that of the Fe^{3+} ion. Apotransferrin (apotf) binds two Al^{3+} ions that compete with the Fe^{3+} ion for the same binding sites.[34] Difference UV studies confirm that the Al^{3+} ion binds to tyrosine side chains,[34,35] and ^{13}C NMR studies have shown that the binding of the Al^{3+} ion involves the binding of a synergistic carbonate anion.[36,37] Last, small-angle X-ray scattering studies indicate that aluminum binding causes an overall protein conformational change that is similar to that caused by iron binding.[38]

The speciation within the LMM fraction of serum aluminum is not well established. Normal serum contains only ~0.1−0.3 μM of aluminum,[6,31,39,40] and contamination from adventitious aluminum is a constant problem. In addition, the LMM complexes are relatively labile, so that the speciation can be altered by separation methods such as electrophoresis. These problems have been reviewed by van Landeghem et al.,[41] who concluded that there is no reliable analytical method for identifying the LMM aluminum complexes in serum.

Because of these difficulties, there have been several attempts to calculate the speciation of aluminum using the stability constants of the Al^{3+} ion with the chelating agents present in serum.[34,42−46] However, these calculations have been hampered by uncertainties regarding the aluminum-binding constants for key serum complexing agents such as citrate (cta) and phosphate.[47] In this study, effective aluminum-binding constants for both phosphate and citrate have been determined at pH 7.4 by direct competition between these ligands and transferrin, using difference UV spectroscopy to monitor the distribution of the aluminum between the ligands and the protein at concentrations that are close to clinical serum aluminum levels. This has produced a new, internally consistent set of binding constants for transferrin, citrate, and phosphate that have been used to assess the relative importance of citrate and phosphate, with respect to the complexation of aluminum in serum.

(11) Doll, R. *Age Aging* **1993**, *22*, 138−153.
(12) Martyn, C. N.; Coggon, D. N.; Inskip, H.; Lacey, R. F.; Young, W. F. *Epidemiology* **1997**, *8*, 281−286.
(13) Yokel, R. A. *Neurotoxicology* **2000**, *21*, 813−828.
(14) Gidden, H.; Holland, F. F.; Klein, E. *Trans.—Am. Soc. Artif. Intern. Organs* **1980**, *26*, 133−138.
(15) Keirsse, H.; Smeyers-Verbeke, J.; Verbeelen, D.; Massart, D. L. *Anal. Chim. Acta* **1987**, *196*, 103−114.
(16) Graf, H.; Stummvoll, H. K.; Meisinger, V.; Kovarik, J.; Wolf, A.; Pinggera, W. F. *Kidney Int.* **1981**, *19*, 587−592.
(17) Leung, F. Y.; Hodsman, A. B.; Muirhead, N.; Henderson, A. R. *Clin. Chem.* **1985**, *31*, 20−23.
(18) Lundin, A. P.; Caruso, C.; Sass, M.; Berlyne, G. M. *Clin. Res.* **1978**, *26*, 636A.
(19) Galbraith, L. V.; Bradley, C.; Krijnen, P. M. W.; Leung, F. Y. *Clin. Chem.* **1988**, *34*, 1304.
(20) Elliot, H. L.; MacDougall, A. I.; Haase, G.; Cumming, R. L. C.; Gardiner, P. H. E.; Fell, G. S. *Lancet* **1978**, 940−941.
(21) Perez Parajon, J.; Blanco González, E.; Cannata, J. B.; Sanz-Medel, A. *Trace Elem. Med.* **1989**, *6*, 41−46.
(22) Blanco González, E.; Perez Parajon, J.; Alonso, J. I. G.; Sanz-Medel, A. *J. Anal. At. Spectrom.* **1989**, *4*, 175−179.
(23) Wróbel, K.; Blanco González, E.; Sanz-Medel, A. *Analyst (Cambridge, U.K.)* **1995**, *120*, 809−815.
(24) Sanz-Medel, A.; Fairman, B. *Mikrochim. Acta* **1992**, *109*, 157−160.
(25) Wróbel, K.; Blanco González, E.; Sanz-Medel, A. *J. Anal. At. Spectrom.* **1994**, *9*, 281−284.
(26) Soldano Cabezuelo, A. B.; Blanco González, E.; Sanz-Medel, A. *Analyst (Cambridge, U.K.)* **1997**, *122*, 573−577.
(27) Sanz-Medel, A.; Soldano Cabezuelo, A. B.; Milacic, R.; Bantan Polak, T. *Coord. Chem. Rev.* **2002**, *228*, 373−383.
(28) Cochran, M.; Patterson, D.; Neoh, S.; Stevens, B.; Mazzachi, R. *Clin. Chem.* **1985**, *31*, 1314−1316.
(29) D'Haese, P. C.; Van Landeghem, G. F.; Lamberts, L. V.; De Broe, M. E. *Mikrochim. Acta* **1995**, *120*, 83−90.
(30) Garcia Alonso, J. I.; Lopez Garcia, A.; Perez Parajon, J.; Blanco González, E.; Sanz-Medel, A.; Cannata, J. B. *Clin. Chim. Acta* **1990**, *189*, 69−79.
(31) Soldano Cabezuelo, A. B.; Blanco González, E.; Garcia Alonso, J. I.; Sanz-Medel, A. *Analyst (Cambridge, U.K.)* **1998**, *123*, 865−869.
(32) Sarra, R.; Garratt, R.; Gorinsky, B.; Jhoti, H.; Lindley, P. *Acta Crystallogr., Sect. B: Struct. Sci.* **1990**, *B46*, 763−771.
(33) MacGillivray, R. T. A.; Moore, S. A.; Chen, J.; Anderson, B. F.; Baker, H.; Luo, Y.; Bewley, M.; Smith, C. A.; Murphy, M. E. P.; Wang, Y.; Mason, A. B.; Woodworth, R. C.; Brayer, G. D.; Baker, E. N. *Biochemistry* **1998**, *37*, 7919−7928.
(34) Harris, W. R.; Sheldon, J. *Inorg. Chem.* **1990**, *29*, 119−124.
(35) Gelb, M. H.; Harris, D. C. *Arch. Biochem. Biophys.* **1980**, *200*, 93−98.
(36) Bertini, I.; Luchinat, C.; Messori, L.; Scozzafava, A.; Pellacani, G.; Sola, M. *Inorg. Chem.* **1986**, *25*, 1782−1786.
(37) Aramini, J. M.; Saponja, J. A.; Vogel, H. J. *Coord. Chem. Rev.* **1996**, *149*, 193−229.
(38) Grossmann, J. G.; Neu, M.; Evans, R. W.; Lindley, P. F.; Appel, H.; Hasnain, S. S. *J. Mol. Biol.* **1993**, *229*, 585−590.
(39) Griswold, W. R.; Reznik, V.; Mendoza, S. A.; Trauner, D.; Alfrey, A. C. *Pediatrics* **1983**, *71*, 56−58.
(40) Bantan, T.; Milacic, R.; Mitrovic, B.; Pihlar, B. *J. Anal. At. Spectrom.* **1999**, *14*, 1743−1748.
(41) Van Landeghem, G. F.; De Broe, M. E.; D'Haese, P. C. *Clin. Biochem.* **1998**, *31*, 385−397.
(42) Dayde, S.; Filella, M.; Berthon, G. *J. Inorg. Biochem.* **1990**, *38*, 241−259.
(43) Duffield, J. R.; Edwards, K.; Evans, D. A.; Morrish, D. M.; Vobe, R. A.; Williams, D. R. *J. Coord. Chem.* **1991**, *23*, 277−290.
(44) Jackson, G. E. *Polyhedron* **1990**, *9*, 163−170.
(45) Venturini, M.; Berthon, G. *J. Inorg. Biochem.* **1989**, *37*, 69−90.
(46) Harris, W. R. *Clin. Chem.* **1992**, *38*, 1809−1818.
(47) Harris, W. R.; Berthon, G.; Day, J. P.; Exley, C.; Flaten, T. P.; Forbes, W. F.; Kiss, T.; Orvig, C.; Zatta, P. *J. Toxicol. Environ. Health* **1996**, *48*, 543−568.

Experimental Section

Materials. Analytical-reagent-grade citric acid and sodium dihydrogen phosphate were purchased and used without further purification. Carbonate-free potassium hydroxide solutions were prepared from Dilut-It ampules, using freshly deionized water. All potassium hydroxide solutions were standardized by titrations of primary standard potassium hydrogen phthalate. The absence of carbonate in the potassium hydroxide solutions was confirmed by Gran's plots.[48] Stock solutions of aluminum were prepared by dissolving the reagent-grade chloride salt in 100 mM hydrochloric acid. The aluminum solutions were standardized by eluting a known volume through a strong cationic exchange column and titrating the eluant with a standardized potassium hydroxide solution. Apotransferrin (apoTf) was purchased from Sigma and purified as previously described.[49] Concentrations of apoTf solutions were determined from the absorbance at 278 nm, using a molar extinction coefficient of 93 000 M^{-1} cm^{-1}.

Difference UV Titrations. All difference UV titrations were performed in 0.1 M *N*-2-hydroxyethylpiperazine-*N*′-ethanesulfonic acid (Hepes) at pH 7.4. The cuvettes were maintained at 25 °C by an external circulating water bath. UV spectra were recorded using a modernized Cary model 14 spectrophotometer that was running the OLIS operating system. The methods for titrating apoTf with anions[49−51] and for titrating a metal−transferrin complex with a chelating agent[52,53] have been reported. A detailed description of the methods is given in the Supporting Information. The only significant difference from previous studies is that two different titrant solutions were used in each experiment. A more dilute titrant was used initially to provide more data points for the early part of the titration, whereas a more concentrated titrant was used near the end of the titration to force the binding reaction toward saturation.

The various binding equilibria involving transferrin, aluminum, and the competing ligands can be described by the general equation

$$i\mathrm{Al}^{3+} + m\mathrm{Tf} + j\mathrm{L} \rightleftarrows \mathrm{Al}^{3+}{}_i\mathrm{Tf}_m\mathrm{L}_j \qquad (1)$$

where L represents the ligand (either citrate or phosphate) and Tf represents transferrin. It is presumed that a synergistic carbonate anion is bound concomitantly with each Al^{3+} ion; however, for simplicity, the carbonate is not shown in eq 1. For each species in the system, there is an effective binding constant, which is defined as

$$\beta^*_{imj} = \frac{[\mathrm{Al}_i\mathrm{Tf}_m\mathrm{L}_j]}{[\mathrm{Al}^{3+}]^i[\mathrm{Tf}]^m[\mathrm{L}]^j} \qquad (2)$$

The asterisk denotes that these are effective binding constants, which are valid only at the experimental pH and bicarbonate concentration. Nonlinear least-squares fits of the difference UV titration data were used to calculate effective binding constants for Al−citrate and Al−phosphate, as described in the Results section.

Potentiometric Titrations. Potentiometric titrations were performed using a thermostated glass titration cell that was maintained at 25 °C by an external circulating water bath. All titrations were performed under an argon atmosphere. The ionic strength of all solutions was adjusted to 0.10 M by the addition of 1.0 M KNO_3. The pH was measured with an Accumet model 25 pH meter equipped with a combination electrode. The pH meter was calibrated as previously described[54] to read the value of $-\log [H^+]$ directly, rather than the hydrogen ion activity.

The titrations were conducted using a computer-controlled autotitrator that added an aliquot of titrant, stirred the contents of the titration cell, and monitored the pH versus time. When the pH drift fell below 0.001 pH unit per minute, the final pH was recorded and the buret was prompted for the next addition of the titrant. In some experiments, the pH drift criterion was set to 0.0005 pH unit per minute; however, this change in the autotitrator settings had no discernible effect on the resulting binding constants. No data point with an equilibration time of >1 h was included in the calculations. A set of ligand protonation constants was determined from titrations of citrate alone. Al−citrate binding constants were obtained from titrations of samples with aluminum concentrations of 1−4 mM and a citrate:Al^{3+} ratio of either 1:1 or 2:1.

The complexation equilibria for the Al−citrate system are described by a set of formal equilibrium constants of the form

$$\beta_{ijk} = \frac{[\mathrm{Al}_i\mathrm{cta}_j\mathrm{H}_k]^{-(3j-3i-k)}}{[\mathrm{Al}^{3+}]^i[\mathrm{cta}^{3-}]^j[\mathrm{H}^+]^k} \qquad (3)$$

where the indices *i*, *j*, and *k* represent the stoichiometric coefficients for the three reactants. The citrate species cta^{3-} in the denominator of eq 3 refers to a free citrate molecule in which all three carboxylate groups are deprotonated. However, citrate binding to the Al^{3+} ion involves coordination and deprotonation of the central alcoholic group. Thus, within an aluminum complex, the trianionic ligand is coordinated via the central carboxylate and alkoxide groups and one terminal carboxylate group, with an uncoordinated terminal carboxylic acid.[55−59] The dangling, terminal carboxylic acid also deprotonates with no change in the Al coordination mode as the pH increases; this form of the ligand is designated as $H_{-1}cta^{4-}$.

Least-Squares Fitting. Both the difference UV data and the potentiometric data were analyzed by a nonlinear least-squares method, using customized versions of the general nonlinear least-squares program ORGLES.[60] Each data set was fit by first defining a model, which consisted of a specific set of complex species, each of which was described by an appropriate binding constant. All models included the set of aluminum hydrolysis constants β_{10-n} of −5.46, −10.04, −15.74, and −23.49 for $n = 1-4$ from Baes and Mesmer[61] as fixed parameters. The quality of each fit was judged by a goodness-of-fit parameter, defined as

$$\mathrm{GOF} = \sqrt{\frac{\sum_1^{n_{\mathrm{obs}}}(Y_n^{\mathrm{obs}} - Y_n^{\mathrm{calc}})^2}{n_{\mathrm{obs}} - n_{\mathrm{p}}}} \qquad (4)$$

where Y^{obs} and Y^{calc} are the observed and calculated values of either

(48) Rossotti, F. J. C.; Rossotti, H. *J. Chem. Educ.* **1965**, *42*, 375−378.
(49) Harris, W. R.; Cafferty, A.; Trankler, K.; Maxwell, A.; MacGillivray, R. T. A. *Biochim. Biophys. Acta* **1999**, *1430*, 269−280.
(50) Harris, W. R.; Nesset-Tollefson, D. *Biochemistry* **1991**, *30*, 6930−6936.
(51) Harris, W. R.; Cafferty, A.; Abdollahi, S.; Trankler, K. *Biochim. Biophys. Acta* **1998**, *1383*, 197−210.
(52) Harris, W. R.; Pecoraro, V. L. *Biochemistry* **1983**, *22*, 292−299.
(53) Harris, W. R. *J. Inorg. Biochem.* **1986**, *27*, 41−52.
(54) Harris, W. R.; Chen, Y.; Stenback, J.; Shah, B. *J. Coord. Chem.* **1991**, *23*, 173−186.
(55) Lakatos, A.; Bányai, I.; Decock, P.; Kiss, T. *Eur. J. Inorg. Chem.* **2001**, 461−469.
(56) Motekaitis, R. J.; Martell, A. E. *Inorg. Chem.* **1984**, *23*, 18−23.
(57) Öhman, L.-O. *Inorg. Chem.* **1988**, *27*, 2565−2570.
(58) Rubini, P.; Lakatos, A.; Champmartin, S.; Kiss, T. *Coord. Chem. Rev.* **2002**, *228*, 137−152.
(59) Martin, R. B. *Clin. Chem.* **1986**, *32*, 1797−1806.
(60) Busing, W. R.; Levy, H. A. *OR GLS, A General Fortran Least Squares Program*; Technical Report No. ORNL-TM-271. Oak Ridge National Laboratory: Oak Ridge, TN, 1962.

absorptivity or pH, n_{obs} is the number of observations, and n_p is the number of adjustable parameters. Both programs used here have been used in several previous studies.[34,50,54,62−64]

Mass Spectrometry Studies. Mass spectra of Al−citrate solutions were recorded on a JEOL model Mstation spectrometer using electrospray ionization−mass spectroscopy (ESI−MS). Spectra were recorded at a mass resolution of 2500, with an accelerator voltage of 5.0 kV, a lens voltage of 73 V, an orifice temperature of 100 °C, and a desolvation temperature of 200 °C. The mass spectrometer was calibrated with CsI.

In one set of experiments, aqueous solutions of 1 mM aluminum trichloride ($AlCl_3$) and either 1 or 2 mM citric acid were mixed and adjusted to a pH value of 2.3−8 by the addition of ammonium hydroxide. The samples were allowed to equilibrate overnight, after which a final solution pH was measured. The equilibrated samples were then filtered through a 0.45 μm syringe filter and introduced into the mass spectrometer by continuous infusion at a rate of 100 μL per minute. Each spectrum was the average of seven scans.

In a second set of experiments, an aqueous aliquot of $AlCl_3$ was added to 20 mL of 500 μM citric acid. The pH was immediately adjusted to 7.4 ± 0.2 with NH_4OH, and mass spectra were recorded as a function of time over a period of several hours. Time-dependent mass spectra were recorded for samples with total aluminum concentrations of 100, 50, and 20 μM.

Results

Anion−Transferrin Binding Constants. Samples of apoTf in 0.1 M Hepes were titrated with both phosphate and citrate, and the resulting families of difference UV spectra are shown in Figures S2 and S3 in the Supporting Information. The spectra were essentially identical with those reported previously for phosphate and several other anions.[65,66] The absorbance of the negative difference UV peak near 245 nm was converted to an absorptivity by dividing the absorbance by the analytical concentration of transferrin. Titration curves were prepared by plotting the absorptivity versus the cumulative concentration of anion in the cuvette and are shown in Figure S4 in the Supporting Information.

Previous studies on anion binding to transferrin have shown that one anion binds to each lobe of apoTf.[51,66] Thus, each anion−transferrin titration curve was fit by a nonlinear least-squares method, using three adjustable parameters: the equilibrium constants for the binding of two anions to the protein (β^*_{011} and β^*_{012}), and the molar absorptivity of the anion−transferrin complex ($\Delta\epsilon_M$). The final set of anion−transferrin binding constants have been converted to the stepwise binding constants $K_1 = \beta^*_{011}$ and $K_2 = \beta^*_{012}/\beta^*_{011}$ and are listed in Table 1.

The titrations of Al−transferrin described below were conducted in the presence of 5 mM carbonate, to duplicate the conditions under which the Al−transferrin binding constants were originally measured. Thus, before the measured anion−transferrin binding constants were included in fitting the Al−transferrin titration data, they were corrected for the presence of carbonate using the procedures previously described.[51] The corrected constants are listed in Table 1.

Table 1. Anion−Apotransferrin Binding Constants

$[HCO_3^-]$ (mM)	log K_1	log K_2	$\Delta\epsilon_M$ (M^{-1} cm^{-1})
	Citrate		
0.17	4.17 ± 0.01	3.78 ±0.02	6800 ± 120
5[a]	3.76	3.37	
	Phosphate		
0.17	3.99 ± 0.01	2.73 ± 0.03	6800 ± 160
5[a]	3.58	2.32	

[a] Constants obtained by adjusting the experimental binding constants from a bicarbonate concentration of 0.17 mM to 5 mM.

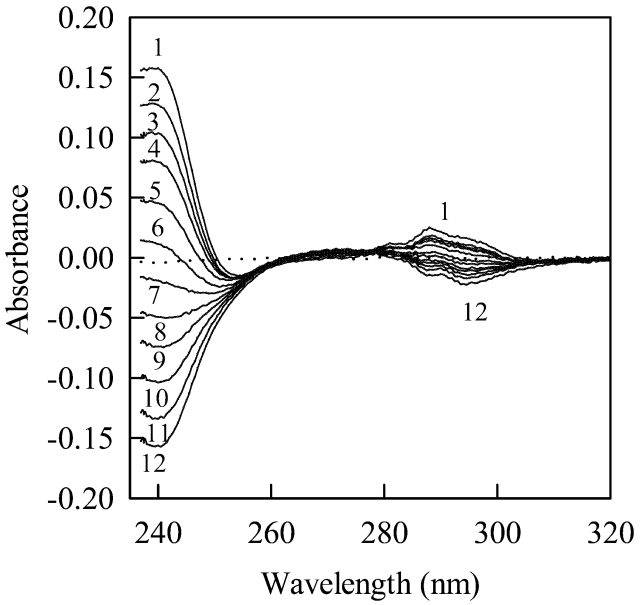

Figure 1. Difference UV spectra generated by the titration of Al−transferrin with citrate in 0.1 M Hepes at pH 7.4. The dotted line is a baseline of apoTf vs apoTf. $[Al^{3+}] = 12$ μM; [ApoTf] = 15 μM. Cumulative concentration of citrate for each spectrum is as follows: curve 1, 0 mM; curve 2, 0.0443 mM; curve 3, 0.0881 mM; curve 4, 0.1316 mM; curve 5, 0.2003 mM; curve 6, 0.2682 mM; curve 7, 0.3433 mM; curve 8, 0.4255 mM; curve 9, 0.5063 mM; curve 10, 0.6250 mM; curve 11, 0.7787 mM; and curve 12, 0.9274 mM.

Titrations of Al−Transferrin with Citrate. The Al−transferrin complex was first formed by the addition of 0.8 equiv of Al^{3+} to apoTf, and then it was titrated with sequential aliquots of citrate to generate the set of difference UV spectra shown in Figure 1.

The aluminum-binding constant of the C-terminal site is approximately a factor of 10 larger than that of the N-terminal site;[34] therefore, most of the aluminum initially binds to the C-terminal site. The initial spectrum shows the positive peak at 240 nm for this Al−transferrin complex. As the titration proceeds, the aluminum is removed from the protein and replaced by citrate, generating the negative difference UV peak of the $(cta)_2$−transferrin complex.

Previous studies have shown that nonsynergistic anions and bicarbonate compete for the same anion-binding sites on apoTf, and they show that occupancy of a site by a nonsynergistic anion prevents metal binding at that site.[51]

(61) Baes, C. F.; Mesmer, R. E. *The Hydrolysis of Cations*; Wiley: New York, 1976.
(62) Harris, W. R.; Chen, Y. *Inorg. Chem.* **1992**, *31*, 5001−5006.
(63) Harris, W. R.; Chen, Y.; Wein, K. *Inorg. Chem.* **1994**, *33*, 4991−4998.
(64) Harris, W. R.; Yang, B.; Abdollahi, S.; Hamada, Y. *J. Inorg. Biochem.* **1999**, *76*, 231−242.
(65) Harris, W. R.; Nesset-Tollefson, D.; Stenback, J. Z.; Mohamed-Hani, N. *J. Inorg. Biochem.* **1990**, *38*, 175−183.
(66) Harris, W. R. *Biochemistry* **1985**, *24*, 7412−7418.

Scheme 1

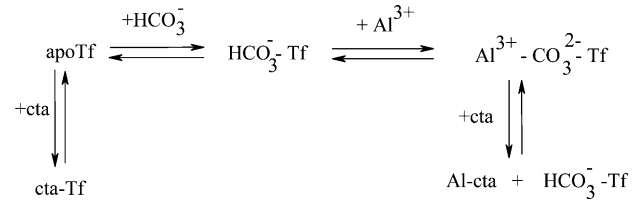

On the basis of these observations, the interactions among citrate, aluminum, and transferrin can be represented by Scheme 1. For simplicity, the scheme represents only one binding site rather than the two sites of apoTf.

The scheme shows that an anionic ligand such as citrate can affect Al−transferrin binding in two ways. One way is by competing with bicarbonate for the anion-binding site, which reduces the concentration of the metal-binding HCO_3−transferrin binary species. The other way is by chelating the metal ion in direct competition with the protein.

To fit the absorbance data from the titration of Al−transferrin with citrate, one has to consider the transferrin complexes Al−transferrin, Al_2−transferrin, cta−transferrin, and $(cta)_2$−transferrin. The binding constants for Al−transferrin and Al_2−transferrin (β^*_{110} and β^*_{210}) for pH 7.4 and 5 mM bicarbonate have been reported previously.[34] The cta−transferrin binding constants (β^*_{011} and β^*_{012}) have been determined as described previously. Thus, these four equilibrium constants serve as fixed constants in the calculations of the Al−citrate binding constants.

When Al is bound to the C-terminal binding site, the N-terminal is still available for binding citrate. Thus, one must include the ternary Al_C−transferrin−cta_N species in the analysis of the difference UV data. (Here, Al_C represents Al bound to the C-terminal binding site, and cta_N represents citrate bound to the N-terminal site.) There is little, if any, cooperativity between metal binding at one site of transferrin and anion binding at the other site.[65] Therefore, a binding constant for the Al_C−transferrin−cta_N ternary complex can be calculated as the product of the site-specific Al−transferrin and citrate−transferrin binding constants.

For a protein with two equivalent binding sites, the site-specific binding constants for the C- and N-terminal binding sites (k_C and k_N, respectively) are related to the experimentally measured macroscopic binding constants (K_1 and K_2) by the equations

$$K_1 = k_C + k_N \tag{5}$$

$$\frac{1}{K_2} = \frac{1}{k_C} + \frac{1}{k_N} \tag{6}$$

On the basis of the reported macroscopic binding constants for aluminum,[34] eqs 5 and 6 give microscopic binding constants of $\log k_C^{Al} = 13.45$ and $\log k_N^{Al} = 12.55$.

For two independent binding sites, statistical factors lead to a minimum separation of 0.6 log units between the log K_1 and log K_2 values. The stepwise macroscopic binding constants for citrate-transferrin are separated by only 0.4 log units. Although this smaller separation could be interpreted as indicating a positive cooperativity in the binding of citrate, it more likely reflects experimental errors. Thus, we assign the microconstant for the binding of the citrate to both the C- and N-terminal binding sites as the average of the stepwise citrate binding constants, which gives $k_{cta} = 10^{3.57}$. The overall binding constant for Al_C−transferrin−cta_N is simply

$$\beta^*_{111} = k_C^{Al} k_{cta} = 10^{17.02} \tag{7}$$

The binding constants for all the transferrin species in the Al−transferrin−cta system can be assigned independently; therefore, the only unknown binding constants are those of the binary Al−cta complexes. The difference UV titrations are conducted at a single pH of 7.4; therefore, it is not possible to differentiate among complexes that differ only in their proton stoichiometry. For example, β^*_{101} represents the cumulative binding of all 1:1 Al:cta complexes, such as Al:cta and $Al(H_{-1}cta)^-$. The initial attempts to fit the titrations of Al−transferrin with cta considered β^*_{101} as well as β^*_{102}, representing $Al(cta)_2$ complexes; β^*_{303}, representing the $Al_3(cta)_3(OH)^{4-}$ trimer; β^*_{202}, representing the dimeric $Al_2(H_{-1}cta)_2^{2-}$ complex proposed by Venturini and Berthon;[45] and β^*_{203}, representing a dinuclear $Al_2(H_{-1}cta)(cta)_2^{4-}$ complex recently characterized by Dakanali et al.[67] The details of the various models that were considered are given in the Supporting Information. The general result was that the least-squares refinement consistently rejected each of the polynuclear complexes whenever β^*_{101} was included in the model. Sequential cycles of least-squares refinement gave a smaller and smaller binding constant for the polynuclear complex until this species no longer represented a significant fraction of the total aluminum. The best fit of the difference UV data was obtained using only β^*_{101}, β^*_{102}, and the $\Delta\epsilon_M$ for cta−transferrin as adjustable parameters. The observed and calculated titration curves for the titration of Al−transferrin with citrate are shown in Figure 2. Despite the complexity of this system, the average GOF for four independent titrations was only 237 M^{-1} cm^{-1}, indicating a very good set of fits. The effective Al−citrate binding constants are listed in Table 2.

Difference UV Titrations of Al−Transferrin with Phosphate. Samples of Al−transferrin were also titrated with phosphate (P_i), and a typical set of difference UV spectra is shown in Figure 3. The initial spectrum is that of the Al−transferrin complex, which is gradually transformed to the negative spectrum of the $(P_i)_2$−transferrin species as the titration proceeds. As with the previously discussed citrate system, the binding constants for all the transferrin species except the β^*_{111} for the Al_C−transferrin−$(P_i)_N$ ternary complex have been measured independently and can be used as fixed values in the least-squares refinement of the phosphate titrations.

β^*_{111} values for the Al_C−transferrin−$(P_i)_N$ complex have been estimated from the microscopic binding constants for aluminum and phosphate, using the method described by eq 7. The macroscopic P_i−transferrin binding constants can be

(67) Dakanali, M.; Raptopoulou, C. P.; Terzis, A.; Lakatos, A.; Banyai, I.; Kiss, T.; Salifoglou, A. *Inorg. Chem.* **2003**, *42*, 252−254.

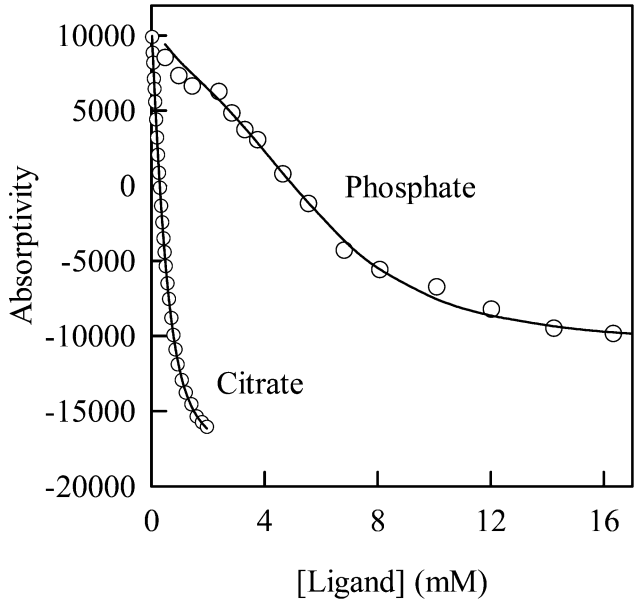

Figure 2. Titrations of Al−transferrin with citrate and phosphate. The symbols represent the actual data, whereas the lines represent the least-squares fits.

Table 2. Effective Aluminum-Binding Constants for Citrate and Phosphate at pH 7.4

	citrate	phosphate
$\log \beta^*_{111}$[a]	17.02	15.79
$\log \beta^*_{101}$	11.59 ± 0.19	
$\log \beta^*_{102}$	14.90 ± 0.55	12.02 ± 0.16
$\Delta\epsilon_M$ (L−Tf) (M^{-1} cm^{-1})	8600 ± 1060	5770 ± 1070
GOF[b] (M^{-1} cm^{-1})	237	707

[a] Fixed parameter calculated from eq 7. [b] Goodness of fit, as defined by eq 4.

used with eqs 5 and 6 to calculate site-specific microconstants of $10^{3.55}$ and $10^{2.34}$ for the binding of phosphate to transferrin. It is not clear which of these constants corresponds to the N-terminal binding site; thus, two possible values for β^*_{111}—$10^{15.79}$ and $10^{17.00}$—were calculated by matching the value of k_C^{Al} for Al−Tf with each of the two phosphate−transferrin microscopic binding constants. Two sets of calculations were performed to determine which value of β^*_{111} gave the best fit of the Al−transferrin titration data.

The initial attempts to fit the data included β^*_{101} and β^*_{102} for the 1:1 and 1:2 aluminum:phosphate complexes and the $\Delta\epsilon_M$ for the P_i−transferrin complex as adjustable parameters. Surprisingly, the refinements consistently reduced the β^*_{101} constant to an insignificant value. Therefore, the titrations of Al−transferrin with phosphate were fit using only β^*_{102} and the phosphate−transferrin $\Delta\epsilon_M$ values as adjustable parameters. Using the lower value of $10^{15.79}$ for β^*_{111}, the average GOF for the phosphate titrations was 609 M^{-1} cm^{-1}. A typical set of titration data and the calculated fit are shown in Figure 2. For the alternative value of $10^{17.00}$, the average GOF increased substantially, to 1730 M^{-1} cm^{-1}. Thus, one clearly obtains a better fit for the smaller value of $\beta^*_{111} = 10^{15.79}$. The final $\log \beta^*_{102}$ value for Al−phosphate was 12.02 ± 0.16 (Table 2).

We could not refine β^*_{101} and β^*_{102} simultaneously; therefore, a second model was tested in which β^*_{102} was discarded and replaced with β^*_{101} as an adjustable parameter. The result was a $\log \beta^*_{101}$ value of 9.62, but the resulting GOF value, 1281 M^{-1} cm^{-1}, was substantially higher than that obtained by varying β^*_{102}. This model attributes all the complexation to the 1:1 complex; thus, the value of 9.62 represents an upper limit on the value of $\log \beta^*_{101}$.

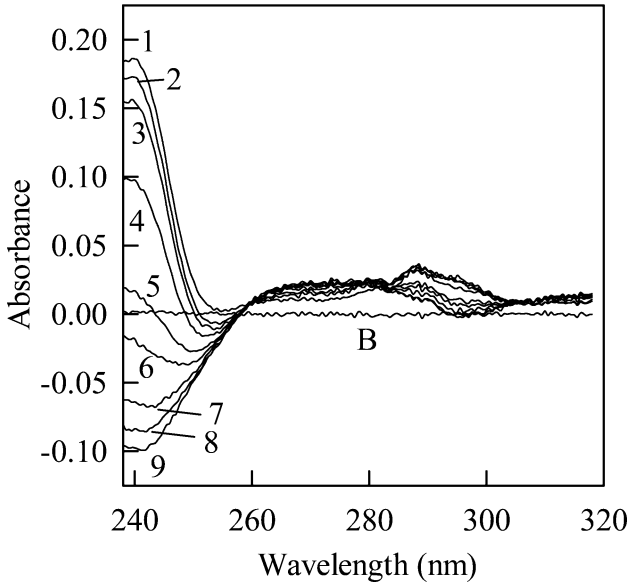

Figure 3. Difference UV spectra generated by the titration of Al−transferrin with phosphate in 0.1 M Hepes buffer at pH 7.4. The cumulative concentration of phosphate for each curve is described as follows: curve B, 0 mM (baseline); curve 1, 0.122 mM; curve 2, 0.846 mM; curve 3, 1.30 mM; curve 4, 1.80 mM; curve 5, 3.64 mM; curve 6, 4.98 mM; curve 7, 7.76 mM; curve 8, 11.35 mM; and curve 9, 16.07 mM.

Al−Citrate Potentiometric Titrations. Solutions of citrate alone, as well as samples with both 1:1 and 2:1 cta:Al ratios were titrated with aliquots of standardized KOH. Titration curves were prepared by plotting the equilibrated pH versus the equivalents of KOH added, as shown in Figure 4. As expected, the free-ligand titration shows one buffer region corresponding to the titration of the three carboxylic acid groups of citric acid. These data were used to calculate citric acid pK_a values of 5.70 ± 0.01, 4.35 ± 0.01, and 2.92 ± 0.01, which agree with literature values for this ligand.[68]

The titration of a 1:1 solution of Al:cta shows one extended buffer region at low pH that terminates with a sharp inflection at 4.33 equiv of base. The position of the inflection indicates that, at neutral pH, essentially all the aluminum is present as the $[Al_3(H_{-1}cta)_3(OH)(H_2O)]^{4-}$ trimer that has been detected in previous titrations[57,69] and has been characterized crystallographically[70] and by NMR.[70−72] As noted previously, $H_{-1}cta^{4-}$ represents a coordinated citrate molecule in which the central alcoholic group, as well as the three carboxylate groups, have been deprotonated.

(68) Martell, A. E.; Smith, R. M. *Critical Stability Constants*; Plenum: New York, 1974.
(69) Öhman, L.-O.; Sjöberg, S. *J. Chem. Soc., Dalton Trans.* **1983**, 2513−2517.
(70) Feng, T. L.; Gurian, P. L.; Healy, M. D.; Barron, A. R. *Inorg. Chem.* **1990**, *29*, 408−411.
(71) Bodor, A.; Bányai, I.; Tóth, I. *Coord. Chem. Rev.* **2002**, *228*, 175−186.
(72) Bodor, A.; Bányai, I.; Zékány, L.; Tóth, I. *Coord. Chem. Rev.* **2002**, *228*, 163−173.

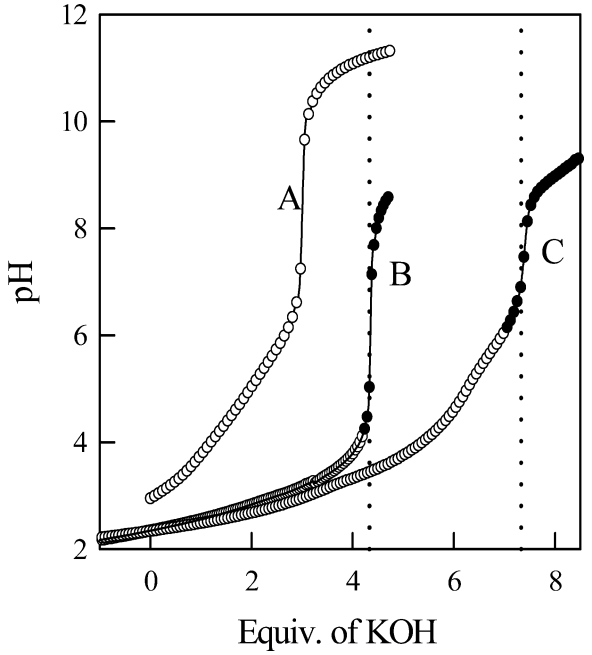

Figure 4. Potentiometric equilibrium curves for the titration of Al−citrate solutions with KOH. Curve A depicts citrate only, whereas curve B represents a 1:1 cta:Al ratio and curve C represents a 2:1 cta:Al ratio. For the titration of citrate only, an equiv unit is defined as one mole of KOH per mole of ligand. For the Al−citrate titrations, an equiv unit is defined as one mole of KOH per mole of aluminum. The vertical lines are drawn at 4.33 and 7.33 equiv, which correspond to the expected location of the inflections assuming the complete formation of the $Al_3(H_{-1}cta)_3OH^{4-}$ trimer. The data shown as filled circles in curve C were omitted from calculations of binding constants, because of persistent drifting in the pH.

The formation of the trimer during the potentiometric titration was confirmed by the ^{27}Al NMR spectrum. The spectrum of the titration sample at pH 7.5 is very similar to that reported previously for the trimer,[70] with one relatively sharp peak located at 1.5 ppm and a second, broader peak located at 12.0 ppm with integrated intensities of 1:2.

The 2:1 titration curve in Figure 4 also shows one buffer region that terminates with a sharp inflection near 7.33 equiv. The position of the inflection is consistent with the release of 4.33 protons due to the complete formation of the trimer, combined with the release of three protons from the titration of 1 equiv of free citric acid. This indicates that, even with a 2:1 excess of ligand, the trimer is essentially the sole Al species in solution at pH 7.

After the addition of ~3 equiv of base, the equilibration times in the 1:1 titrations increased to ~25 min per point, even though no precipitation was observed. The complete titration required ~10 h. For the 2:1 titrations, the equilibration times were much shorter, typically <5 min per point, through the addition of ~7.1 equiv of base, so that the titrations could be completed in ~5 h. Because of the differences in the equilibration times, we have more confidence in the data from the 2:1 titrations, and all the binding constants reported in this paper are based only on the 2:1 titrations. All the pH values up to the addition of ~7.1 equiv of base were used in the calculations of binding constants.

Various combinations of species have been tested to find the model that best fits the potentiometric data. All the models included the 1:1 complexes $Al(Hcta)^+$ and Al(cta), the 2:1 complexes $Al(cta)_2^{3-}$ and $Al(cta)(H_{-1}cta)^{4-}$, and the well-established trimer $Al_3(H_{-1}cta)_3(OH)^{4-}$. Attempts were made to add $Al(H_{-1}cta)^-$, $Al(H_{-1}cta)(OH)^{2-}$, $Al_2(H_{-1}cta)_2^{2-}$, $Al_2(cta)_3^{3-}$, and $Al_2(H_{-1}cta)(cta)_2^{4-}$ to these core species. The results of these calculations are included in the Supplemental Information. There was no strong evidence for including $Al(H_{-1}cta)(OH)^{2-}$ or $Al(H_{-1}cta)(cta)_2^{4-}$. Good fits could be obtained by including any one of the species $Al(H_{-1}cta)^-$, $Al_2(H_{-1}cta)_2^{2-}$, or $Al_2(cta)_3^{3-}$; however, it was impossible to include more than one of these complexes.

To reduce the number of adjustable parameters in the refinement of the potentiometric data, the difference UV results were used to determine a value for the binding constant of $Al(H_{-1}cta)^-$. The value of β^*_{101} is the sum of the effective binding constants of all 1:1 Al−citrate complexes, as shown in eq 8:

$$\beta^*_{101} = \beta_{111}[H] + \beta_{110} + \frac{\beta_{11-1}}{[H]} + \frac{\beta_{11-2}}{[H^+]^2} \qquad (8)$$

where the effective binding constant β^*_{101}, as determined from difference UV titrations, is defined in eq 2 and the formal stability constants on the right-hand side of eq 8 are defined in eq 3. Given that β^*_{101} is $10^{11.59}$, it was clear from the preliminary calculations and from previous studies[45,56,57,73,74] that neither β_{111} nor β_{110} makes a significant contribution to β^*_{101} at pH 7.4. It was not clear how to partition the effective binding constant between β_{11-1} and β_{11-2}. At one extreme, if the effective binding is due solely to $Al(H_{-1}cta)^-$, then $\log \beta_{11-1} = 4.19$. Conversely, if the binding at pH 7.4 is due solely to $Al(H_{-1}cta)(OH)^{2-}$, then $\log \beta_{11-2} = -3.21$. The potentiometric data have been refined using each of these constants, and one obtains virtually identical GOF values.

It seems more logical to include $Al(H_{-1}cta)^-$ rather than adopt a model in which Al(cta) loses two protons simultaneously to go directly to $Al(H_{-1}cta)(OH)^{2-}$. Furthermore, in models where β_{11-2} is fixed at $10^{-3.21}$, speciation calculations show that there would be no significant formation of the $Al(H_{-1}cta)(OH)^{2-}$ complex under the conditions of the potentiometric titrations. Therefore, we have accepted the $\log \beta_{11-1}$ value of 4.19 for use in analyzing the potentiometric data. Two potentiometric models, one including β_{22-2} and another that includes β_{230} have been evaluated, and the results are shown in Table 3. The quality of the least-squares fit is virtually identical for the two models. Based on the mass spectrometry results shown below, the 22−2 model is believed to be the better choice.

Al−Citrate Electrospray Mass Spectrometry. Mass spectra were recorded for solutions matching the potentiometric samples, i.e., 1 mM of Al and either 1 or 2 mM of citrate. The solution species were protonated during the ionization process, so that they were detected as either mono- or dianions in the mass spectrum, regardless of their original

(73) Gregor, J. L.; Powell, H. K. J. *Aust. J. Chem.* **1986**, *39*, 1851−1864.
(74) Jackson, G. E. *S. Afr. J. Chem.* **1982**, *35*, 89−92.

Table 3. Al−Citrate Binding Constants from the Use of Different Models To Fit Potentiometric Titrations of 2:1 cta:Al Solutions

	22−2 model	230 model
$\log \beta_{111}$[a]	10.66 ± 0.09	10.68 ± 0.09
$\log \beta_{110}$	8.40 ± 0.04	8.41 ± 0.04
$\log \beta_{11-1}$[b]	4.19	4.19
$\log \beta_{120}$	13.56 ± 0.15	13.64 ± 0.14
$\log \beta_{12-1}$	7.65 ± 0.38	7.83 ± 0.26
$\log \beta_{22-2}$	12.12 ± 0.12	
$\log \beta_{230}$		25.04 ± 0.17
$\log \beta_{33-4}$	16.15 ± 0.42	16.15 ± 0.37
GOF[c]	0.0081	0.0075

[a] β_{ikj} is defined by eq 3. [b] This constant is not allowed to vary during the least-squares refinement. [c] Goodness of fit, as defined by eq 4.

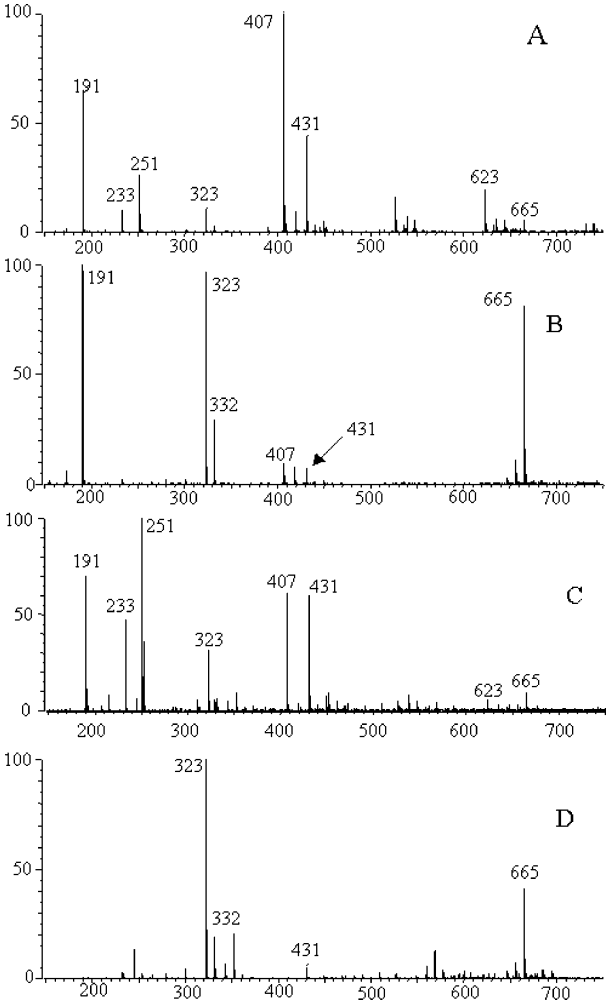

Figure 5. Electrospray mass spectra for Al−citrate solutions ((A) 1 mM $AlCl_3$, 2 mM citrate, pH 2.54; (B) 1 mM $AlCl_3$, 2 mM citrate, pH 7.1; (C) 1 mM $AlCl_3$, 1 mM citrate, pH 2.58; and (D) 1 mM $AlCl_3$, 1 mM citrate, pH 6.6).

charge in solution. For example, citric acid was always observed as the H_2cta^{-1} species at *m*/*z* 191, even at pH values where cta^{3-} was the form present in solution. Thus, no effort has been made to use the mass spectra to distinguish between species that differ only in their degree of protonation, such as $Al(cta)_2^{3-}$ versus $Al(H_{-1}cta)(cta).^{4-}$ Although no alkali metals were added to any of these samples, the spectra of a citrate blank also showed several citrate clusters with Na^+ and K^+ ions. These included peaks at *m*/*z* 405 $Na(H_2cta)_2^-$, *m*/*z* 421 $K(H_2cta)_2^-$, and *m*/*z* 651 $K,Na(H_2cta)_3^-$.

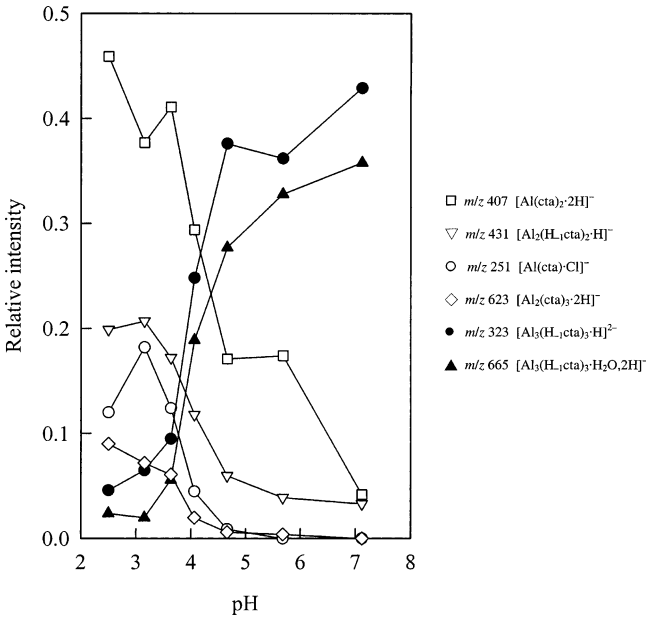

Figure 6. Plot of relative peak intensity in electrospray mass spectra as a function of pH for solutions with 1 mM of $AlCl_3$ and 2 mM of citrate.

The electrospray ionization mass spectrum of a 1:2 Al:cta solution at pH 2.54 is shown in Figure 5A. At this pH, one would expect a mixture of $Al(Hcta)^+$, $Al(cta)^0$, and a small amount of $Al(H_{-1}cta)^-$. The peak at *m*/*z* 233 corresponds to the gas-phase species $[Al(H_{-1}cta)\cdot H_2O]^-$ and the peak at *m*/*z* 251 corresponds to $[Al(cta)\cdot Cl]^-$. The largest peak is located at *m*/*z* 407, which corresponds to $[Al(cta)_2\cdot 2H]^-$. Figure 5A also shows a significant peak at *m*/*z* 431, which can be assigned to the dimeric $[Al_2(H_{-1}cta)_2\cdot H]^-$ anion, and a smaller peak at *m*/*z* 623 for the dinuclear $[Al_2(cta)_3\cdot 2H]^-$ anion.

Protonation of the Al−citrate trimer to a monoanion would give an *m*/*z* value of 665 for the gas-phase species $[Al_3(H_{-1}cta)_3\cdot H_2O,2H]^-$. There is only a small peak at 665 at pH 2.5, but this peak increases substantially as the pH increases (vide infra). In addition, there is a peak at *m*/*z* 323, which we can assign to the dianionic complex $[Al_3(H_{-1}cta)_3\cdot H]^{2-}$. The 2− charge for this species is indicated by the appearance of the $m + 1$ peak at a half-integer *m*/*z* value. The peaks at *m*/*z* 323, 323.5, and 324 have relative intensities 1:0.23:0.07, which agree very well with values of 1:0.21:0.07, which were calculated on the basis of the ^{13}C content of three citrate ligands.

The mass spectrum of a 1:2 Al:cta solution at pH 7.1 is shown in Figure 5B. The Al−citrate trimer peaks at *m*/*z* 323 and 665 have become the major peaks in the spectrum, whereas a marked reduction is observed in the peaks of the mononuclear 1:1 species at *m*/*z* 233 and the 1:2 complex at *m*/*z* 407. Another peak has emerged at *m*/*z* 332, which can be assigned as an second dianionic trimer peak corresponding to $[Al_3(H_{-1}cta)_3\cdot H_2O,H]^{2-}$, on the basis of the isotope pattern of peaks at 332, 332.5, and 333 with relative ratios of 1:0.2:0.06.

The mass spectra easily track the conversion of monomeric Al−citrate to the trimer as the pH increases, as shown in Figure 6. The monomeric 1:1 and 1:2 species, represented

by peaks at *m*/*z* 251 and 407, decrease as the pH increases. The concentration of the $Al_2(H_{-1}cta)_2^{2-}$ dimer follows the same pH dependence as the monomers. In contrast, the trimer, which is represented by peaks at *m*/*z* 323 and 665, increases as the pH increases and becomes the dominant species at pH >5.

The mass spectrum for a solution containing 1 mM of aluminum and 1 mM of citrate at pH 2.58 is shown in Figure 5C. Compared to the 2:1 cta:Al solutions previously described, there are substantial increases in the peaks at *m*/*z* 251 and 233 that are associated with the 1:1 complexes and an increase in the peak at *m*/*z* 431 due to the $Al_2(H_{-1}cta)_2^{2-}$ dimer. The peak for the $Al(cta)_2^{3-}$ species is reduced but is still significant despite the 1:1 metal:ligand ratio. The spectrum of a 1:1 solution at pH 6.6 is shown in Figure 5D. At this higher pH, the peak of the bis(citrate) complex at *m*/*z* 407 is completely gone, and only small peaks are observed for the monomer at *m*/*z* 233 and the dimer at *m*/*z* 431. The major peaks are the trimer peaks at *m*/*z* 323 and 665.

The mass spectroscopy data indicate that, when there is a 2:1 cta:Al ratio, the potentiometric samples contain a mixture of the $Al(H_{-1}cta)^-$ monomer, the $Al_2(H_{-1}cta)_2^{2-}$ dimer, and the dinuclear $Al_2(cta)_3^{3-}$ complex. The mass spectroscopy signal for the dimer is consistently larger than that for $Al_2(cta)_3^{3-}$; therefore, we believe that the 22−2 model shown in Table 3 is the better description of the potentiometric results.

The mass spectra of solutions containing 500 μM of citrate and 100, 50, and 20 μM of aluminum were also examined for peaks at *m*/*z* 431, corresponding to the $Al_2(H_{-1}cta)_2^{2-}$ dimer and at *m*/*z* 623, representing the $Al_2(cta)_3^{3-}$ complex. There were small peaks at *m*/*z* 431 in solutions with 100 μM and 50 μM of aluminum; however, no peak at *m*/*z* 431 was observed at 20 μM of aluminum. A small peak at *m*/*z* 623 was observed upon preparation of the 100 μM aluminum solution, but this peak disappeared after ∼2 h of equilibration. No peak at *m*/*z* 623 was observed for solutions with either 50 or 20 μM of aluminum.

Rate of Al−Citrate Trimer Formation. The formation of the $Al_3(H_{-1}cta)_3(OH)^{4-}$ trimer is rather slow, even at millimolar concentrations of aluminum and citrate.[55,57] This suggested that, under the dilute conditions of the UV experiments, the formation of the trimer might be too slow for this species to form during the ∼4 h time period of the titration. To address this issue, the rate of trimer formation was monitored by electrospray mass spectrometry. Mass spectra were recorded as a function of time for solutions of 500 μM of citrate at pH 7.4 with either 100, 50, or 20 μM of aluminum. These initial spectra show the rapid formation of the monomeric 1:1 species (*m*/*z* 233 and 251) and the 2:1 complex (*m*/*z* 407), with relatively small peaks for the trimer. No internal standard was available; therefore, it was not possible to track absolute concentrations. The rate of conversion of monomers to the trimer is illustrated in Figure 7 by plotting the ratio of *m*/*z* 665 to *m*/*z* 407. At each concentration of aluminum, this ratio rises to a constant value, which is taken to be an indicator that equilibrium has been reached. Each plot in Figure 7 can be fit to a single-exponential function to give an apparent first-order rate constant for the formation of the trimer.

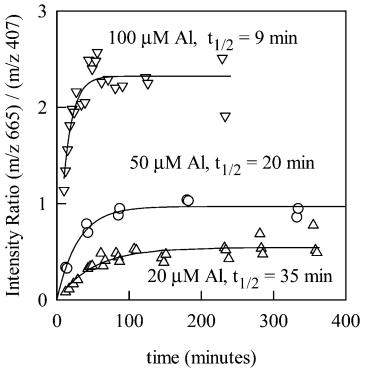

Figure 7. Plots of the ratio of the peak intensities of *m*/*z* 665 to those of *m*/*z* 407, as a function of time for pH 7.4 solutions with 500 μM of citrate and either (▽) 100, (○) 50, or (△) 20 μM of $AlCl_3$.

The apparent half-life for the formation of the trimer increases as the concentration decreases. Under the conditions of the difference UV experiment, a maximum concentration of 7 μM of Al−citrate forms at ∼500 μM of citrate. A linear extrapolation of the half-lives in Figure 7 to 7 μM gives a half-life of ∼80 min for the formation of the trimer.

Discussion

Speciation of Low-Molecular-Mass (LMM) Al−Citrate. There have been numerous potentiometric studies on the complexation of aluminum by citrate.[45,55−57,69,73−75] The Al−citrate system can be titrated over a wide pH range without obvious precipitation; however, there are regions of pH in which very long equilibration times are involved. Because of the slow kinetics and the complexity of the system, there is rather poor agreement among the various published studies. This is the first study to incorporate difference UV and mass spectroscopy data into the analysis of Al−citrate speciation.

a. High Aluminum Concentrations. Most previous potentiometric studies have included the species $Al(Hcta)^+$, Al(cta), $Al(H_{-1}cta)^-$, $Al(cta)_2^{3-}$, and $Al(H_{-1}cta)(cta)^{4-}$. However, Venturini and Berthon[45] preferred the $Al_2(H_{-1}cta)_2^{2-}$ dimer over the $Al(H_{-1}cta)^-$ monomer, and they reported a log β_{22-2} value of 12.69 for $\mu = 0.15$ and 37 °C. The mass spectrometric analysis of millimolar Al−citrate solutions reported here indicates the presence of both the monomer and the dimer, as well as a dinuclear complex with a 2:3 Al:cta ratio (Figure 6). On the basis of consideration of both the GOF of the potentiometric data and the relative peak intensities in the mass spectrum, we feel that the 22−2 model in Table 3, which includes the $Al_2(H_{-1}cta)_2^{2-}$ dimer with a log β_{22-2} value of 12.12, represents the best description of the Al−citrate system. This is the first potentiometric study to include both the monomer and the dimer for Al^{3+}. An $Fe_2(H_{-1}cta)_2^{2-}$ complex, and $Cu_2(cta)_2^{2-}$ and $Cu_2(H_{-1}cta)_2$ dimers, have been reported in previous potentiometric studies.[76−79]

(75) Findlow, J. A.; Duffield, J. R.; Williams, D. R. *Chem. Speciation Bioavailability* **1990**, *2*, 3−32.
(76) Timberlake, C. F. *J. Chem. Soc.* **1964**, 5078−5085.

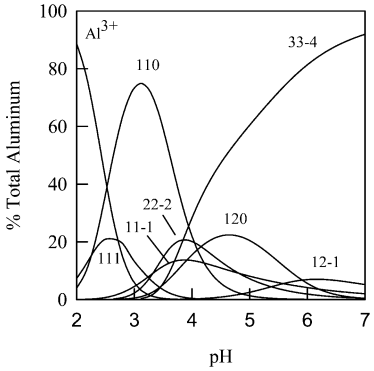

Figure 8. Speciation calculated using the 22−2 model from Table 3. The curves are labeled with the *ijk* stoichiometric coefficients for Al, cta, and H^+, respectively (see eq 3). For example, the curve labeled 111 refers to the Al(Hcta) complex.

The potentiometric and mass spectroscopy data reported here cannot establish the structure of the $Al_2(H_{-1}cta)_2^{2-}$ dimer. However, crystal structures of $M_2(H_{-1}cta)_2$ complexes have been reported for both Fe^{3+} and VO^{2+}.[80,81] Each metal in the dimer has an octahedral coordination geometry involving two carboxylates and the alkoxide group from one citrate plus the alkoxide and one carboxylate from the other citrate. The sixth coordination site is occupied by water for the ferric complex and the oxo ligand in the vanadyl complex. It seems likely that the structure for $Al_2(H_{-1}cta)_2^{2-}$ will be very similar to that of $Fe_2(H_{-1}cta)_2^{2-}$.

The calculated species distribution based on the 22−2 model is presented in Figure 8. The fraction of aluminum present as $Al(H_{-1}cta)^-$ and as $Al_2(H_{-1}cta)_2^{2-}$ is a maximum at pH 3.8, with 20% present as the dimer and 14% present as the monomer. Both species decline as the pH increases above 4, because of the growing predominance of the trimer and bis(citrate) complexes. In the alternative 230 model, the only change in the speciation is that the $Al_2(cta)_3^{3-}$ species accumulates over the same pH range as that for the $Al_2(H_{-1}cta)_2^{2-}$ complex, to a maximum of 11% at pH 3.8. There were only minor changes in the concentrations of the remaining species shown in Figure 8.

The potentiometric models in Table 3 include two bis(citrate) complexes: $Al(cta)_2^{3-}$ and $Al(H_{-1}cta)(cta).^{4-}$ Three previous potentiometric studies have reported a second chelate deprotonation reaction to give $Al(H_{-1}cta)_2^{5-}$, with an average pK_a of ∼7.3.[45,55,82] Inspection of Figure 8 reveals why the $Al(H_{-1}cta)_2^{5-}$ species is not observed in this study. The $Al(H_{-1}cta)(cta)^{4-}$ species accumulates to a maximum of only 7% at pH 6.2. Given a pK_a value of 7.3 for this complex, the fraction of aluminum present as the deprotonated $Al(H_{-1}cta)_2^{5-}$ complex would not have exceeded 3% within the pH range used in the calculations, because of the dominance of the trimer as the pH increases.

One can relate the effective binding constant for the 2:1 complexes at pH 7.4 to the formal stability constants, as shown in eq 9.

$$\beta^*_{102} = \beta_{120} + \frac{\beta_{12-1}}{[H^+]} + \frac{\beta_{12-2}}{[H^+]^2} \qquad (9)$$

The experimental value of β^*_{102} determined in this study is $10^{14.90}$. The values β_{120} and β_{12-1} from the 22−2 model give a value of $10^{15.06}$ for the summation on the right-hand side of eq 9, in good agreement with the difference UV results without including any value for β_{12-2}. This suggests that the pK_a value for the formation of $Al(H_{-1}cta)_2^{5-}$ is >7.3.

Both the $Al(H_{-1}cta)(cta)^{4-}$ and $Al(H_{-1}cta)_2^{5-}$ complexes have been isolated and characterized crystallographically.[77,83] Each citrate binds as a tridentate ligand through two carboxylates and the alkoxide group, with one terminal carboxylate remaining uncoordinated. In the $Al(H_{-1}cta)(cta)^{4-}$ complex, one of the uncoordinated carboxylate groups has been protonated. These studies appear to have taken advantage of the slow rate of the trimerization process and isolated the $Al(H_{-1}cta)_2^{5-}$ species quickly enough to avoid the trimer. Indeed, when this isolated 2:1 complex is redissolved at neutral pH, it slowly converts to the trimer.[83]

b. Low Aluminum Concentrations. Speciation calculations were repeated for 10 μM of aluminum and 1 mM of citrate using both the 22−2 model and the 230 model. The results confirm that, at the low aluminum concentration that is characteristic of the difference UV experiments, neither of these dinuclear complexes would be formed. Thus, the lack of any dinuclear aluminum complexes in the model used to fit the difference UV titrations is not a concern. However, the simulations showed that, during the difference UV experiments, one would have expected the trimer to accumulate to a maximum of ∼35% of the total aluminum at a citrate concentration of 500 μM. The calculated trimer concentration decreases to 6% at the end of the titration as the higher citrate concentration shifts the equilibrium to the bis(citrate) complex. The absence of the trimer in the difference UV experiments is attributed to the slow rate of formation of this complex at micromolar aluminum concentrations, as shown in Figure 7.

Al−Phosphate Speciation. There are very serious limitations to the study of the Al−phosphate system by potentiometric methods. The very low solubility of $Al(PO_4)$ leads to precipitation at ∼pH 3.5.[43,84] Thus, most studies collect data only up to pH 3−4, which makes it even more difficult to assess the Al−phosphate binding affinity at physiological pH values. Four different potentiometric studies[42,43,84,85] show

(77) Matzapetakis, M.; Raptopoulou, C. P.; Terzis, A.; Lakatos, A.; Kiss, T.; Salifoglou, A. *Inorg. Chem.* **1999**, *38*, 618−619.
(78) Vañura, P.; Kuca, L. *Collect. Czech. Chem. Commun.* **1978**, *43*, 1460−1475.
(79) Rajan, K. S.; Martell, A. E. *J. Inorg. Nucl. Chem.* **1967**, *29*, 463−471.
(80) Shweky, I.; Bino, A.; Goldberg, D. P.; Lippard, S. J. *Inorg. Chem.* **1994**, *33*, 5161−5162.
(81) Tsaramyrsi, M.; Kaliva, M.; Salifoglou, A.; Raptopoulou, C. P.; Terzis, A.; Tangoulis, V.; Giapintzakis, J. *Inorg. Chem.* **2001**, *40*, 5772−5779.
(82) Van de Vyver, F. L.; Silva, F. J. E.; D'Haese, P. C.; Verbeuken, A. H.; De Broe, M. E. *Contrib. Nephrol.* **1987**, *55*, 198−220.
(83) Matzapetakis, M.; Kourgiantakis, M.; Dakanali, M.; Raptopoulou, C. P.; Terzis, A.; Lakatos, A.; Kiss, T.; Banyai, I.; Mavromoustakos, T.; Salifoglou, A. *Inorg. Chem.* **2001**, *40*, 1734−1744.
(84) Atkári, K.; Kiss, T.; Bertani, R.; Martin, R. B. *Inorg. Chem.* **1996**, *35*, 7089−7094.
(85) Jackson, G. E.; Voyi, K. V. V. *S. Afr. J. Chem.* **1988**, *41*, 17−21.

a wide variation in the results, even for complexes that form at acidic pH.

Because of these severe problems with experimental studies of Al−phosphate near neutral pH, efforts have been made to use linear free-energy relationships (LFERs) to estimate binding constants for $Al(PO_4)$ and $Al(PO_4)(OH)^-$. In 1992, Harris[46] used LFERs to estimate values of $\log \beta_{110} = 14.35$ and $\log \beta_{11-1} = 8.37$. Atkári et al.[84] recently measured several new stability constants for a series of phosphonic acids and were thus able to construct a more credible set of LFERs and reported two possible values of $\log \beta_{110}$—13.5 and 11.3—and a value of 7.2 for $\log \beta_{11-1}$.

The analysis of the difference UV titrations with phosphate (Figure 2) indicates that the upper limit for β^*_{110}, the effective binding constant representing all 1:1 complexes, is $10^{9.62}$. If this binding is attributed entirely to $Al(PO_4)$, then one can set an upper limit of $\log \beta_{110} < 13.8$. Alternatively, one could attribute all the binding to $Al(PO_4)(OH)^-$ and set an upper limit of $\log \beta_{11-1} < 6.37$. It is quite clear that both the values of β_{11-1} estimated from LFERs [46,84] are too large. Of the three estimates for β_{110}, only the lowest value of $10^{11.3}$, reported by Aktári et al.[84], is consistent with the direct competition results. Speciation calculations that included this value of β_{110} indicated that this 1:1 complex would have accumulated a maximum of only 0.1% of the total aluminum during the difference UV titrations. This would obviously have been undetectable in the least-squares refinement.

Low-Molecular-Mass (LMM) Ligands in Serum. It is clear from the titration curves in Figure 2 that citrate is much more effective than phosphate, in regard to removing aluminum from transferrin. Normal serum contains 1.1 mM of phosphate, compared to only 100 μM of citrate.[46] Speciation calculations using the effective binding constants listed in Tables 1 and 2 indicate that 100 μM of citrate will remove ~18% of the aluminum from transferrin, whereas 1.1 mM of phosphate will remove only ~1.4% of the aluminum.

A review of published computer simulations of the speciation of aluminum in serum shows that these studies have given very conflicting results.[47] Some studies predicted that citrate would be the main LMM ligand,[43,86,87] whereas others predict that phosphate would be the more important LMM aluminum binding agent.[42,44,46] There are several difficulties associated with these simulations. The calculations rely on a combination of citrate- and phosphate-binding constants measured from separate studies. Because of the limited pH range of some of the studies, it is often necessary to calculate aluminum speciation at pH 7.4, on the basis of stability constants measured at much lower pH values. Last, the experimental studies typically use millmolar aluminum concentrations, which are 1000-fold greater than physiologically relevant levels.

All these difficulties are reduced in the difference UV competition studies reported here. The effective binding constants for both Al−citrate and Al−phosphate have been determined at an experimental pH of 7.4 and ~10 μM of total aluminum. This is the first case in which constants for both ligands have been determined within a single study using a common reference ligand. Thus, these data are particularly well-suited for evaluating the relative binding affinities of citrate and phosphate.

Simple speciation calculations for 3 μM of aluminum, using the new constants and physiological concentrations of transferrin, citrate, and phosphate, suggest that ~93% of the total aluminum would be bound to transferrin. Of the pool of LMM aluminum, ~88% of the aluminum would be bound to citrate, 8% would be bound to hydroxide, and only ~2% would be bound to phosphate. These new calculations are consistent with several previous analyses of aluminum in serum that have suggested that citrate is the primary LMM chelating agent in serum.[23,87−90] They are also consistent with more-recent fractionation studies that indicate that ~90% of the total serum aluminum is protein bound.[21−27]

We previously published an equilibrium model for the speciation of aluminum in serum that was based on the LFER estimates described above for $\log \beta_{110}$ and $\log \beta_{11-1}$ for Al−phosphate.[46] This model indicated that the LMM component of serum was comprised of 80% $Al(PO_4)(OH)^-$ and only 10% $Al(H_{-1}cta)$. As noted previously, the new results reported here show that these estimated constants are much too high. Thus, the previous speciation model is incorrect.

Recent studies using fast protein liquid chromatography to fractionate serum appear to have detected ternary aluminum−citrate−phosphate complexes,[27,40,91] and Lakatos et al.[92] reported binding constants for four ternary complexes. We are preparing a complete serum model for aluminum speciation that will consider ternary complexes as well as the competition from Ca^{2+} and Mg^{2+} cations for binding to citrate. Despite these remaining uncertainties, it is now seems clear that citrate is the major LMM ligand for aluminum in serum.

Conclusions

Difference UV competition experiments in which phosphate and citrate are used to remove aluminum directly from serum transferrin definitively establish that citrate is the more effective aluminum-binding agent at neutral pH. Speciation calculations that consider the relative concentrations of these ligands in serum confirm that citrate will be the predominant low-molecular-mass ligand for aluminum in serum. The detailed speciation of Al−citrate as a function of pH is still somewhat ambiguous, because it is very difficult to clearly identify a unique speciation model solely on the basis of potentiometric data. Electrospray mass spectroscopy data suggest that, at lower pH, the potentiometric solutions contain

(86) Clevette, D. J.; Orvig, C. *Polyhedron* **1990**, *9*, 151−161.
(87) Öhman, L.-O.; Martin, R. B. *Clin. Chem.* **1994**, *40*, 598−601.
(88) van Ginkel, M. F.; van der Voet, G. B.; van Eijk, H. G.; de Wolff, F. A. *J. Clin. Chem. Clin. Biochem.* **1990**, *28*, 459−463.
(89) Sanz-Medel, A. *Analyst (Cambridge, U.K.)* **1995**, *120*, 799−807.
(90) Bell, J. D.; Kubal, G.; Radulovic, S.; Sadler, P. J.; Tucker, A. *Analyst (Cambridge, U.K.)* **1993**, *118*, 241−244.
(91) Bantan Polak, T.; Milacic, R.; Mitrovic, B.; Benedik, M. *J. Pharm. Biomed. Anal.* **2001**, *26*, 189−201.
(92) Lakatos, A.; Evanics, F.; Dombi, G.; Bertani, R.; Kiss, T. *Eur. J. Inorg. Chem.* **2001**, 3079−3086.

a mixture of 1:1 and 1:2 monomeric aluminum:citric acid (Al−cta) complexes, as well as a 2:2 Al:cta dimer and a small amount of a 2:3 dinuclear Al:cta complex, whereas a 3:3 trimer dominates at neutral pH. The best overall model for Al−citrate was obtained using the difference UV results to set the value for β_{11-1} and calculating values of β_{111}, β_{110}, β_{120}, β_{12-1}, β_{22-2}, and β_{33-4} from the potentiometric data.

Acknowledgment. This work was supported in part by the University of Missouri Research Board (under Grant No. S-3-40454) and the National Institutes of Health (NIH) (under Grant No. HL66227). The authors would like to thank Dr. R. E. K. Winter and Mr. Joe Kramer for collecting the electrospray mass spectrometry data.

Supporting Information Available: UV spectra of transferrin species, methods for difference UV titrations, difference UV spectra and titration curves for anion binding, and the equilibrium models tested in the refinements of the difference UV and potentiometric data. This material is available free of charge via the Internet at http://pubs.acs.org.

IC026027W